

## Supporting Information

# Insight into the mechanism of the water-gas shift reaction over Au/CeO<sub>2</sub> catalysts using combined *operando* spectroscopies

Marc Ziemba<sup>1</sup>, M. Verónica Ganduglia-Pirovano<sup>2</sup>, Christian Hess<sup>1\*</sup>

<sup>1</sup>Eduard-Zintl-Institut für Anorganische und Physikalische Chemie, Technische Universität Darmstadt, Alarich-Weiss-Str. 8, 64287 Darmstadt, Germany

\*christian.hess@tu-darmstadt.de

<sup>2</sup>Instituto de Catálisis y Petroleoquímica-Consejo Superior de Investigaciones Científicas, Marie Curie 2, 28049 Madrid, Spain

**DFT Calculations.** The (110)-, (111)- and (100)-oriented CeO<sub>2</sub> surfaces were modelled using supercells with seven, nine and eleven atomic layers, respectively, with calculated cubic CeO<sub>2</sub> bulk lattice constant ( $a=5.484 \text{ \AA}$ )<sup>1</sup> and a vacuum layer of at least 10 Å. The choice in the number of atomic layers for each surface is based on the convergence of the calculated surface energy. To model the oxygen-terminated CeO<sub>2</sub>(100) surface, half of the oxygen atoms at the surface were removed in a checkerboard style, because of the polarity of the surface.<sup>2</sup> The CeO<sub>2</sub>(110) surface was modeled employing unit cells with (1×1), (2×1) and (2×2) periodicities and (6 × 4 × 1), (3 × 4 × 1) and (3 × 2 × 1) k-point meshes, respectively, selected using the Monkhorst–Pack method.<sup>3</sup> Similarly, for the CeO<sub>2</sub>(100) surface, unit cells with c(1 × 1) and c(2 × 2) periodicities and (4 × 4 × 1) and (2 × 2 × 1) k-meshes, respectively were employed. The surface unit cell and the bottom trilayer were kept fixed during geometry optimization, whereas the rest of the atoms were allowed to fully relax.

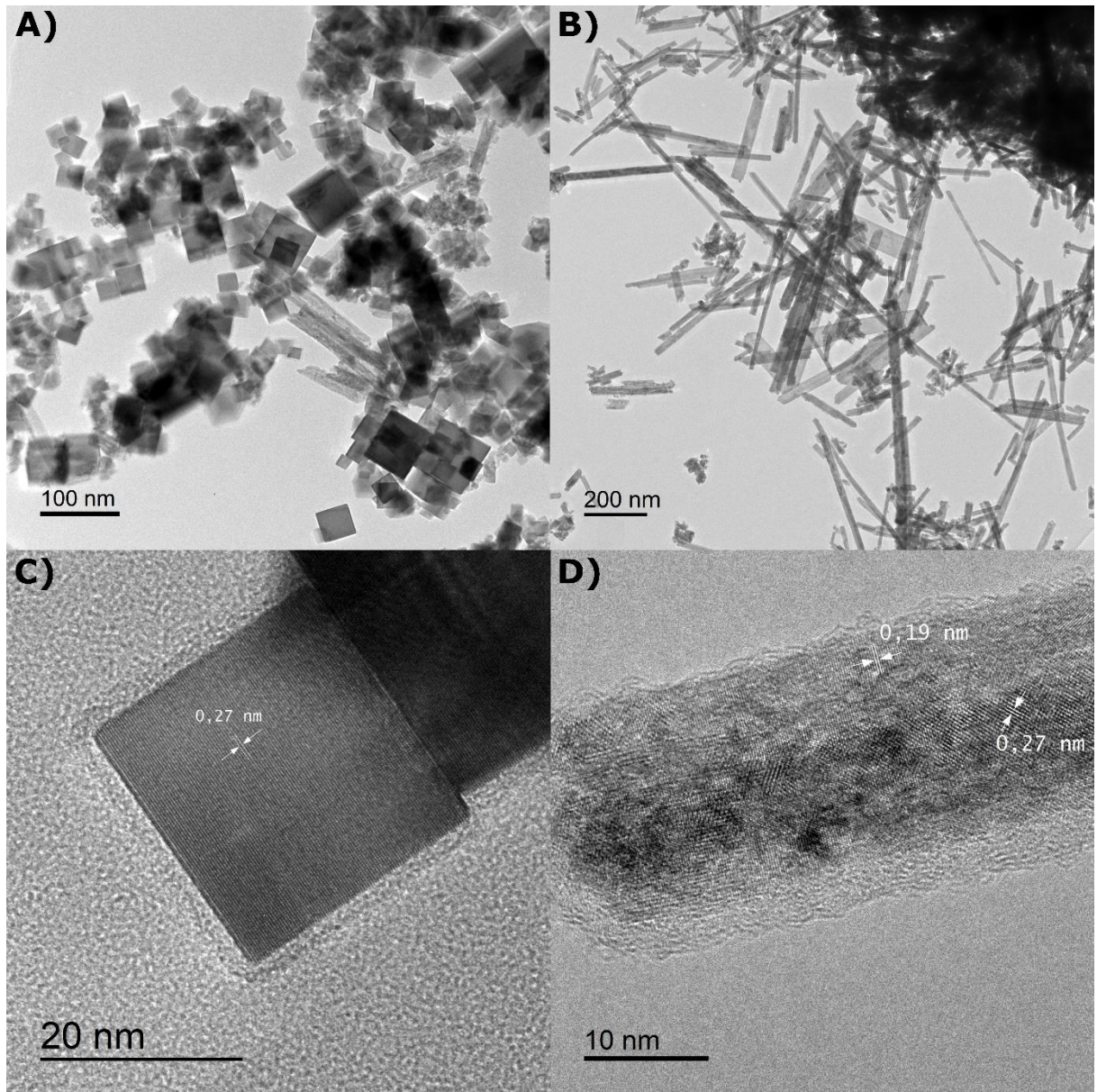


**Figure 1:** TEM images of the synthesized ceria cubes (A), C) and ceria rods (B), D) rods. The white arrows indicate the distance of the lattice planes in the direction of the particle surface.

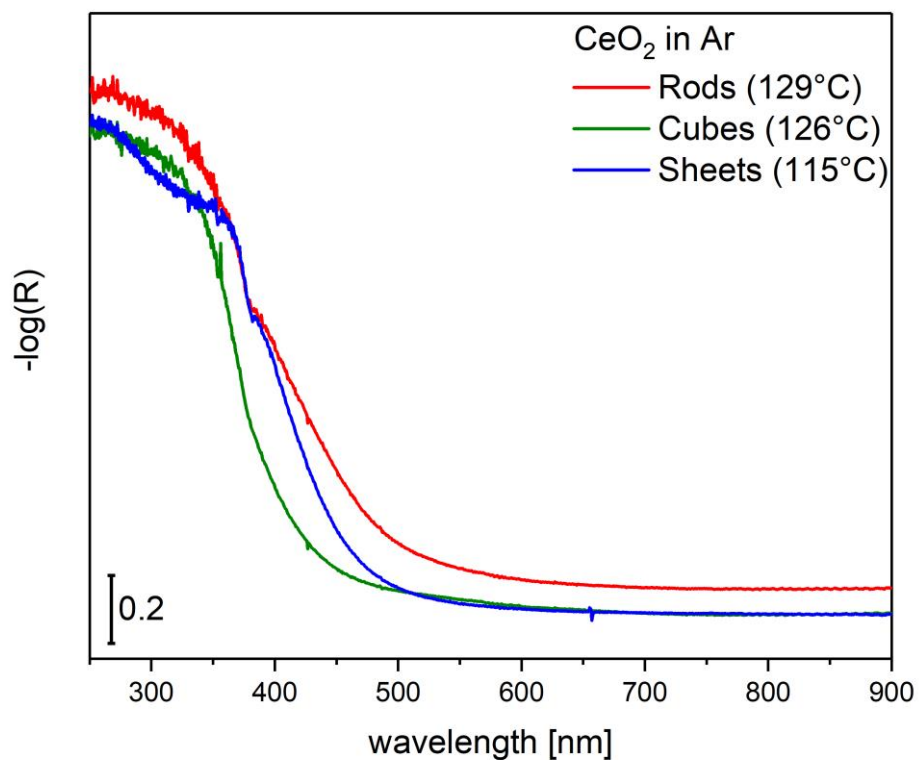


**Figure S2:** *In situ* UV-Vis spectra of the bare CeO<sub>2</sub> samples in Ar flow at 100 mL/min at the indicated temperatures, before exposure to reaction conditions. Spectra correspond to CeO<sub>2</sub> sheets (blue), CeO<sub>2</sub> cubes (green), and CeO<sub>2</sub> rods (red).

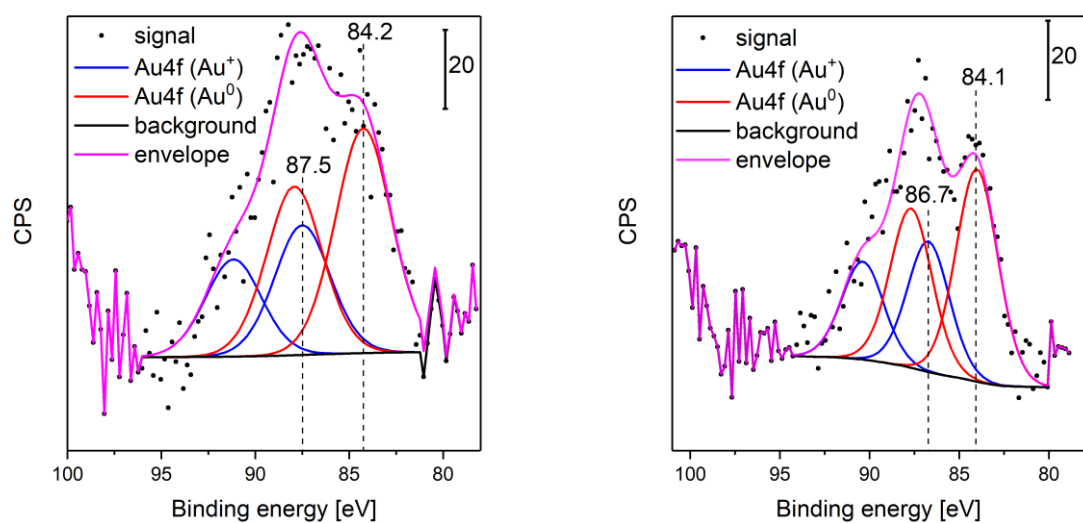


**Figure S3:** Au4f photoemission of the ceria rods loaded with 0.3 wt% Au (left) and 0.5 wt% Au (right). Data is represented by black dots and the background as black line. The fitting

analysis yields contributions from cationic (blue) and metallic (red) gold, and the resulting envelope is given in magenta. For clarity, the positions of the Au4f<sub>7/2</sub> signals are indicated.

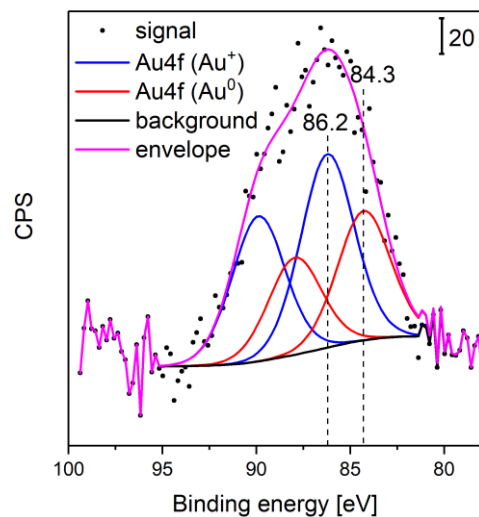


**Figure S4:** Au4f photoemission of the ceria cubes loaded with 0.6 wt% Au. Data is represented by black dots and the background as black line. The fitting analysis yields contributions from cationic (blue) and metallic (red) gold, and the resulting envelope is given in magenta. For clarity, the positions of the Au4f<sub>7/2</sub> signals are indicated.

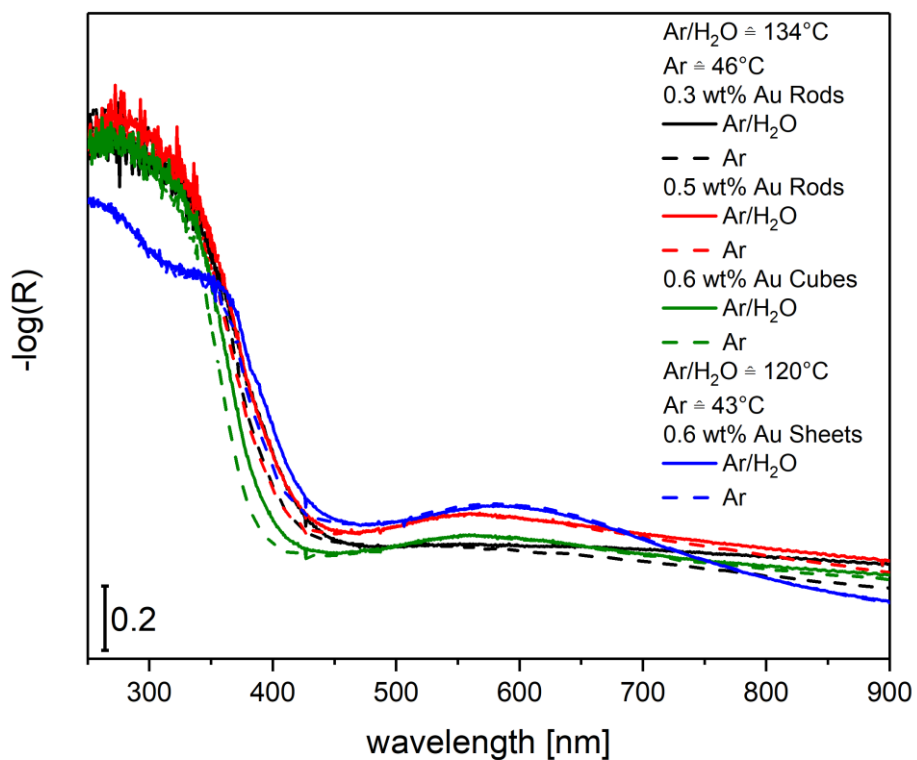


**Figure S5:** *In situ* UV-Vis spectra of the Au/CeO<sub>2</sub> catalysts in H<sub>2</sub>O/Ar (solid lines) and Ar (dashed lines) at a total flow of 100 mL/min and at the indicated temperatures, after exposure to reaction conditions. Spectra correspond to 0.6 wt% Au/CeO<sub>2</sub> sheets (blue), 0.6 wt% Au/CeO<sub>2</sub> cubes (green), 0.3 wt% Au/CeO<sub>2</sub> rods (black), and 0.5 wt% Au/CeO<sub>2</sub> rods (red).

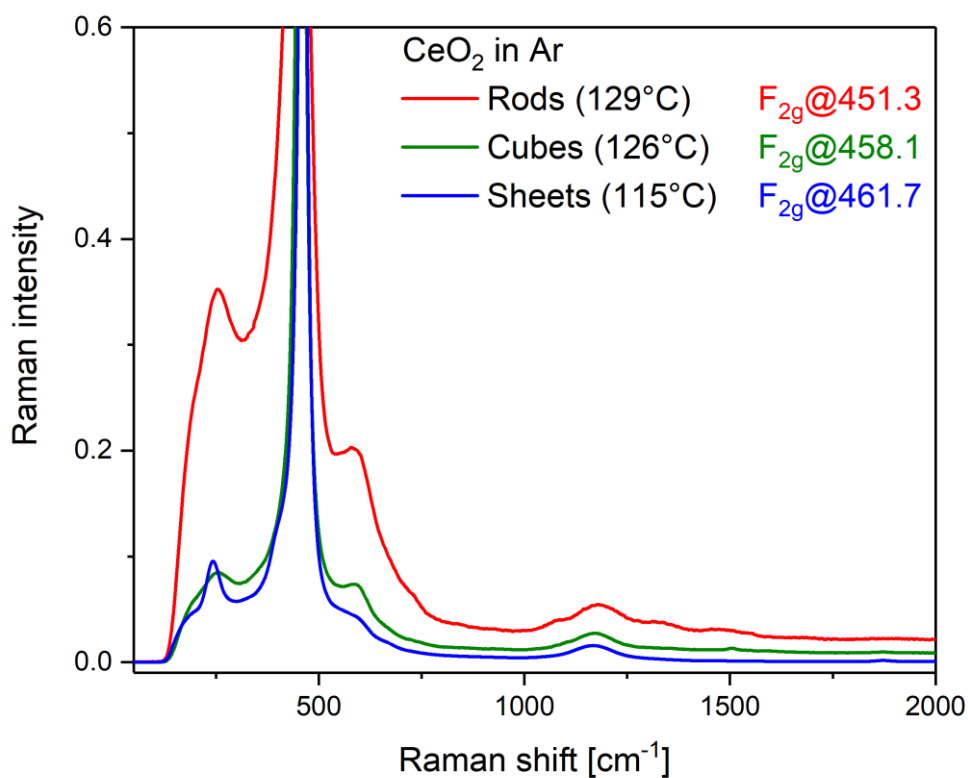


**Figure S6:** *In situ* Raman spectra recorded in Ar flow before switching to reaction conditions. The total flow rate was 100 mL/min, and the temperatures are indicated. The F<sub>2g</sub> bands are cut off for clarity; the F<sub>2g</sub> band positions are given at the top right. Spectra correspond to CeO<sub>2</sub> sheets (blue), CeO<sub>2</sub> cubes (green), and CeO<sub>2</sub> rods (red). Spectra were recorded at 532 nm excitation.

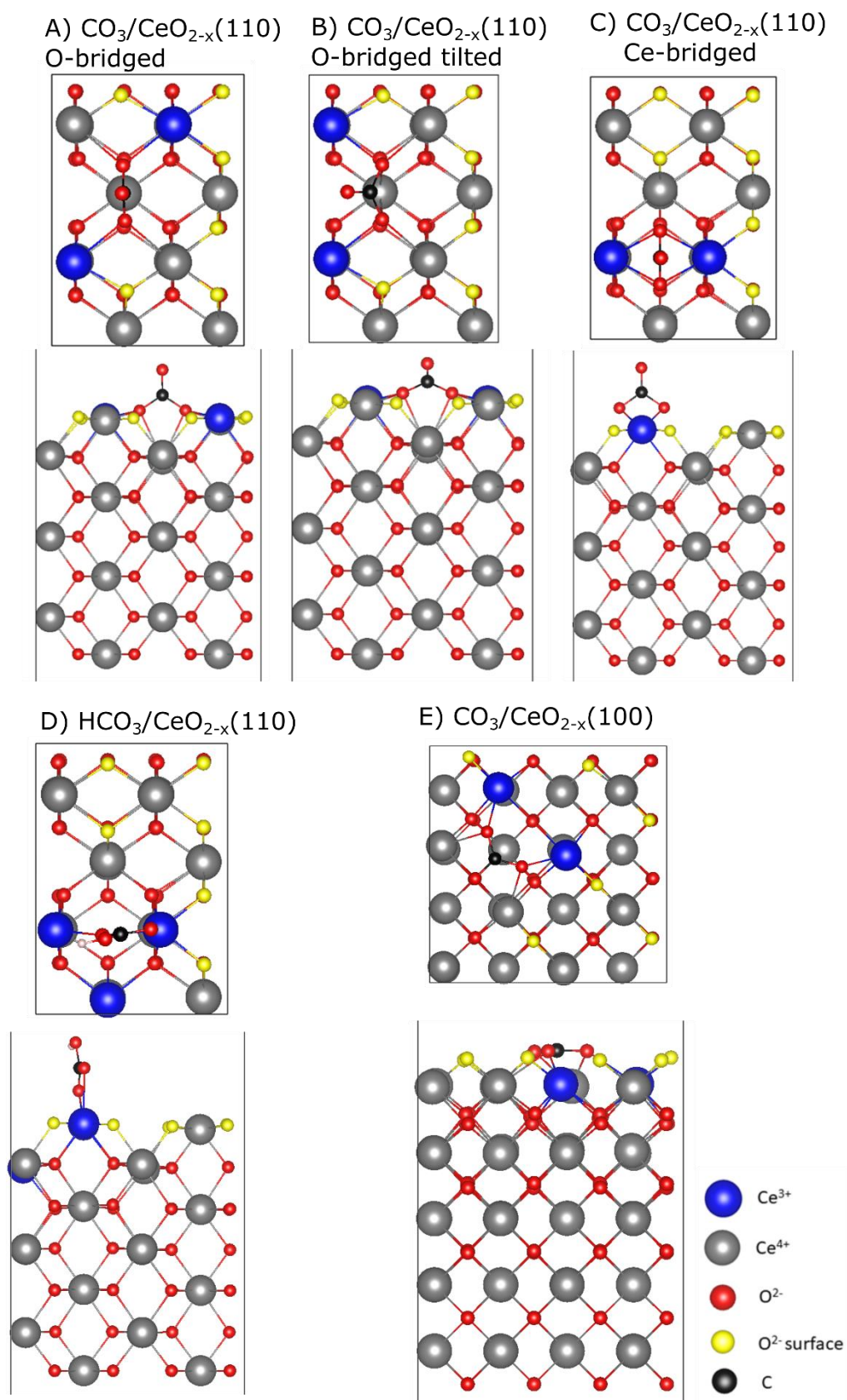


**Figure S7:** Carbonate species on A) to C)  $\text{CeO}_2(110)$ , and D) on  $\text{CeO}_2(100)$  with top and side view with a  $(2 \times 2)$  and a  $c(2 \times 2)$  periodicity, respectively. Atoms correspond to  $\text{Ce}^{3+}$  (blue),  $\text{Ce}^{4+}$  (grey),  $\text{O}^{2-}$  (red), surface  $\text{O}^{2-}$  (yellow), C (black), and H (white).



**Table S1:** Total energies  $E_{\text{tot}}$  and Raman shifts for carbonates on  $\text{CeO}_2(110)$  and  $\text{CeO}_2(100)$  with  $(2 \times 2)$  and  $c(2 \times 2)$  periodicity, respectively. The carbonate vibrations correspond to  $\nu(\text{CO})$ ,  $\nu(\text{CO}_{2,\text{lattice, asym}})$ , and  $\nu(\text{CO}_{2,\text{lattice, sym}})$ . In the case of hydrogen carbonate, the vibrational frequencies correspond to the following vibrations:  $\nu(\text{OH})$ ,  $\nu(\text{OCO, asym})$ ,  $\nu(\text{OCO, sym})$ ,  $\delta(\text{OCOH})$ , and  $\nu(\text{CO}_3, \text{sym})$ .  $E_{\text{ads}}$  is given with respect to  $E_{\text{H}_2} = -6.760$  eV and  $E_{\text{CO}} = 14.806$  eV. Total energies for clean surfaces correspond to  $-678.362$  eV for  $\text{CeO}_2(110)-(2 \times 2)$  and  $-959.603$  eV for  $\text{CeO}_2(100)-c(2 \times 2)$ .

Structure	$E_{\text{tot}} / \text{eV}$	$E_{\text{ads}} / \text{eV}$	Raman shift / $\text{cm}^{-1}$
A) $\text{CO}_3/\text{CeO}_{2-x}(110)^{\text{a}}$	-696.743	-3.574*	1657, 1149, 992
B) $\text{CO}_3/\text{CeO}_{2-x}(110)^{\text{a}}$	-696.713	-3.544*	1571, 1225, 1020
C) $\text{CO}_3/\text{CeO}_{2-x}(110)^{\text{b}}$	-695.151	-1.982*	1665, 1077, 944
D) $\text{HCO}_3/\text{CeO}_{2-x}(110)$	-698.192	-1.643**	3688, 1648, 1353, 1172, 1006
E) $\text{CO}_3/\text{CeO}_{2-x}(100)$	-979.081	-4.672*	1435, 1378, 1053

$$*E_{\text{ads}} = E_{\text{CO}_3/\text{CeO}_{2-x}(110)} - E_{\text{CO}} - E_{\text{CeO}_2(110)}$$

$$**E_{\text{ads}} = E_{\text{HCO}_3/\text{CeO}_{2-x}(110)} - 0.5 E_{\text{H}_2} - E_{\text{CO}} - E_{\text{CeO}_2(110)}$$

<sup>a</sup>One imaginary frequency ( $< 21 \text{ cm}^{-1}$ ).

<sup>b</sup>Two imaginary frequencies ( $< 18 \text{ cm}^{-1}$ ).

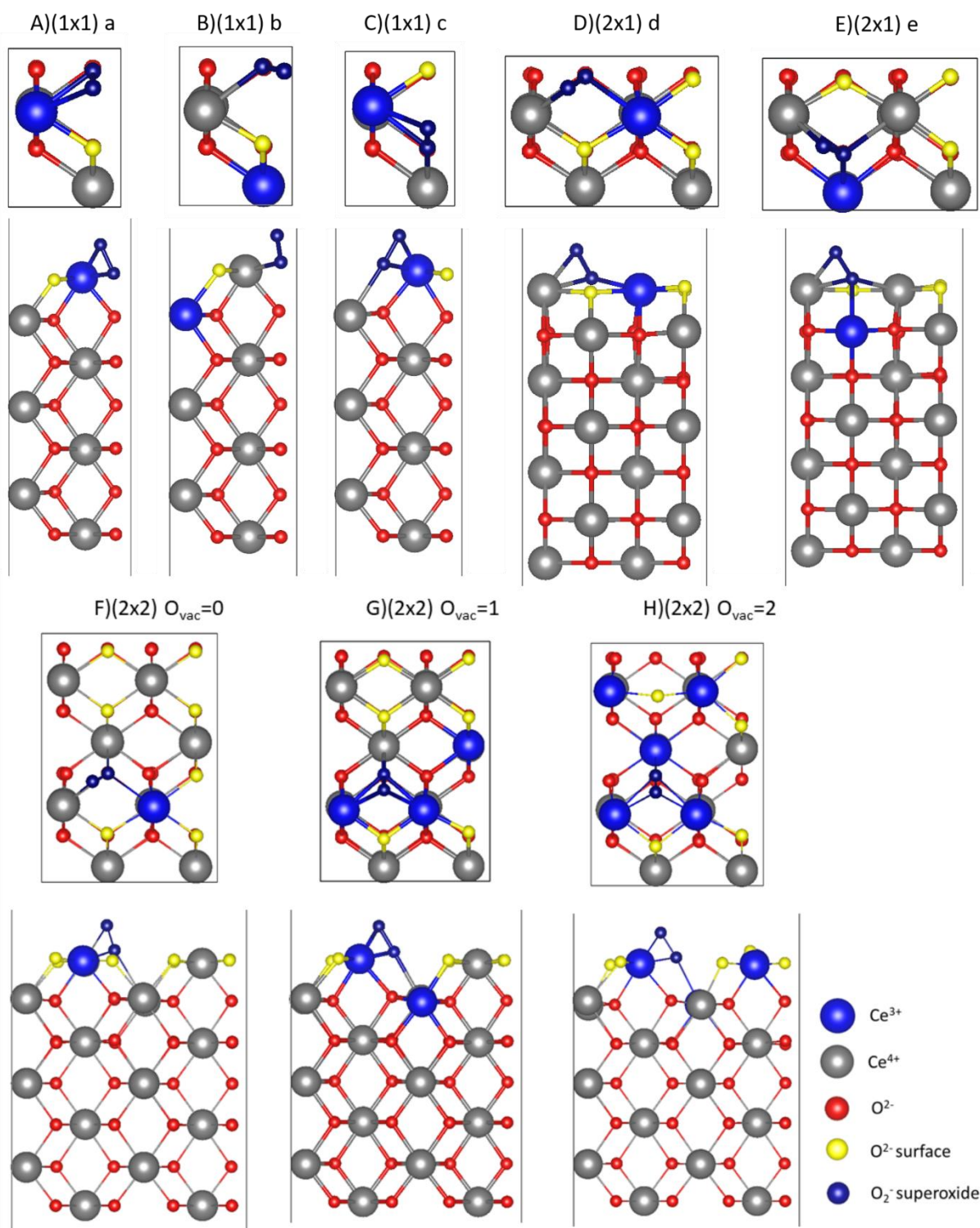


**Figure S8:**  $\text{CeO}_2(110)$  unit cells with top and side view of the most stable superoxide species on the  $\text{CeO}_2(110)$  facet with **A) to C)** (1x1) -, **D) and E)** (2x1) - and **F) to H)** (2x2) periodicity. Atoms correspond to  $\text{Ce}^{3+}$  (blue),  $\text{Ce}^{4+}$  (grey),  $\text{O}^{2-}$  (red), surface  $\text{O}^{2-}$  (yellow), and  $\text{O}_2^-$  (dark blue).

**Table S2:** Total energies  $E_{\text{tot}}$  for superoxides on the  $\text{CeO}_{2-x}(110)$  surface with  $(1\times 1)$ ,  $(2\times 1)$ , and  $(2\times 2)$  periodicities. Furthermore, the average atomic oxygen adsorption energy  $E_{\text{ads},\text{O}}$  for superoxides is given with respect to  $E_{\text{O}_2} = -9.879$  eV. In addition, ML (monolayer) indicates the coverage of the superoxides on the surface, where the value one corresponds to a complete monolayer. The O-O bond length of the superoxide and the Raman shifts are also shown in the Table. Total energies for clean surfaces correspond to  $-169.590$  eV ( $1\times 1$ ),  $-339.180$  eV ( $2\times 1$ ), and  $-678.362$  eV ( $2\times 2$ ).

Structure	Cov. / ML	$E_{\text{tot}}$ / eV	$E_{\text{ads},\text{O}}^*$	O-O bond length / Å	Raman shift / $\text{cm}^{-1}$
$(1\times 1)$ a <sup>a</sup>	0.5	-173.773	0.757	1.418	971
$(1\times 1)$ b	0.5	-173.831	0.698	1.390	1017
$(1\times 1)$ c	0.5	-173.895	0.635	1.404	1004
$(2\times 1)$ d	0.25	-343.588	0.531	1.395	995
$(2\times 1)$ e	0.25	-343.522	0.598	1.395	1001
$(2\times 2)$ $\text{O}_{\text{vac}} = 0$	0.125	-682.759	0.543	1.395	933
$(2\times 2)$ $\text{O}_{\text{vac}} = 1$	0.125	-675.781	0.694	1.421	975
$(2\times 2)$ $\text{O}_{\text{vac}} = 2$	0.125	-669.522	-	1.421	986

<sup>a</sup>One imaginary frequency ( $27 \text{ cm}^{-1}$ ).

$$*E_{\text{ads},\text{O}} = E_{\text{O}_2^-/\text{CeO}_{2-x}(110)} - 0.5 E_{\text{O}_2} - E_{\text{CeO}_2(110)}$$

## References

- 1 C. Schilling, A. Hofmann, C. Hess and M. V. Ganduglia-Pirovano, *J. Phys. Chem. C*, 2017, **121**, 20834–20849.
- 2 N. V. Skorodumova, M. Baudin and K. Hermansson, *Phys. Rev. B*, 2004, **69**, 075401.
- 3 H. J. Monkhorst and J. D. Pack, *Phys. Rev. B*, 1976, **13**, 5188–5192.